

Investigation of Thermal Nonequilibrium on Hypersonic Boundary-Layer Transition by DNS

Jens Linn and Markus J. Kloker

Abstract High-temperature gas effects are known as the physical processes which result in a deviation of the behavior of the calorically perfect gas in the hypersonic-flow regime. These effects may have a significant impact on laminar-turbulent transition of the boundary layer, and thus affect the heat loads of hypersonic vehicles. In the present paper we deal with thermal effects, i.e. rotational and vibrational energy relaxation. A fundamental-breakdown scenario of a Mach-6.8 flat-plate boundary layer at flight conditions is simulated by high-order DNS using a calorically perfect gas, or thermal equilibrium, or a nonequilibrium model. A similar behavior is found for the calorically perfect gas and the thermal equilibrium case. In contrast, a stabilizing effect is observed in the thermal nonequilibrium case, leading to a fall off of fundamental breakdown.

1 Gas Models

The Navier-Stokes Equations are altered in two ways to deal with thermal nonequilibrium (TNEQ), i.e. rotational and vibrational energy relaxation. First, a bulk viscosity or volumetric viscosity μ_v^* is added [3] to approximately account for rotational relaxation. Secondly, a vibrational-energy equation for each species has been added. In this case we deal with two temperatures. The translational temperature is $T^* = T^{*tra}$ and the vibrational temperature T_i^{*vib} for each species, where the superscript $*$ denotes dimensional quantities. The definition of the internal energy now reads:

$$\begin{aligned} e^* &= e^{*trans} + e^{*rot} + e^{*vib} \\ &= \frac{3}{2} \mathcal{R}^* T^* + \mathcal{R}^* T^* + \sum_i c_i \cdot e_i^{*vib}, \text{ with } e_i^{*vib} = \frac{\mathcal{R}_i^* \cdot \theta_i^{*vib}}{\exp(\theta_i^{*vib}/T_i^{*vib}) - 1}, \end{aligned} \quad (1)$$

Institut für Aero- und Gasdynamik, Universität Stuttgart, Pfaffenwaldring 21, D-70550 Stuttgart, GERMANY · e-mail: linn@iag.uni-stuttgart.de; kloker@iag.uni-stuttgart.de

where \mathcal{R}^* is the specific gas constant, $\theta_i^*{}^{vib}$ the characteristic vibrational temperature of the species, and c_i is the mass fraction of species i . The vibrational energy for each species i is modelled by the Landau-Teller equation [3]:

$$\frac{\partial e_i^*{}^{vib}}{\partial t^*} + \nabla \cdot \left(e_i^*{}^{vib} \vec{u}^* \right) + \frac{1}{\tau_i^*{}^{vib}} \left(e_i^*{}^{vib} - e_i^*{}^{vib,eq} \right) = \text{div} \left[\vartheta_i^*{}^{vib} \cdot \nabla T_i^*{}^{vib} \right], \quad (2)$$

where $e_i^*{}^{vib,eq} = e_i^*{}^{vib,eq}(T)$ is the vibrational energy in equilibrium and $\tau_i^*{}^{vib}$ is the relaxation time. A detailed description of the rotational and vibrational energy relaxation models can be found in [3].

Calorically perfect gas (CPG) In the case of CPG the specific heat c_v^* is constant with temperature, and vibrational excitation is neglected. Equation (1) simplifies to:

$$e^* = \frac{3}{2} \mathcal{R}^* T^* + \mathcal{R}^* T^* = \frac{5}{2} \mathcal{R}^* T^* = c_v^* T^* \quad , \quad (3)$$

with $e^*{}^{vib} = 0$; μ_v^* can be turned on or off.

Thermal equilibrium (TEQ) In the thermal equilibrium case, the relaxation time $\tau_i^*{}^{vib}$ tends to zero, hence the term $1/\tau_i^*{}^{vib} \cdot (e_i^*{}^{vib} - e_i^*{}^{vib,eq})$ is dominating eq. (2) and leading the numerical time-step limit of the whole set of equations. Alternatively, the vibrational temperature $T_i^*{}^{vib}$ is set to the translational temperature T^* , with eq. (2) discarded. Test DNS have shown virtually identical results for $\tau_i^*{}^{vib}$ small enough.

Thermal nonequilibrium (TNEQ) Equation (2) is solved employing an algebraic equation for the relaxation time $\tau_i^*{}^{vib}$ as given by Anderson [1]. Thus the temperatures can be different, and the bulk viscosity model is applied:

$$\mu_v^* = \lambda^* + \frac{2}{3} \mu^* \quad , \quad \text{with} \quad \frac{\mu_v^*(T^*)}{\mu^*(T^*)} = \left(\frac{\mu_v^*}{\mu^*} \right)_{T=293.3K} \cdot \exp \left(\frac{T^* - 293.3}{1940} \right) \quad , \quad (4)$$

where λ^* is the coefficient of bulk viscosity (Lamé's constant); μ_v^* scales the dilatation effect, i.e. the term $\mu_v^* \text{div}(\vec{u}^*)$ is added to the normal stresses underlying Stokes' hypothesis.

2 Results

The DNS is based on 6th-order compact finite differences in streamwise and wall-normal directions, with the spanwise derivatives computed by a Fourier ansatz [2, 4]. For the investigation of the rotational and vibrational energy relaxation for a fundamental breakdown scenario, we simulate a Mach-6.8 flat-plate boundary layer at atmospheric flight conditions as investigated by Fezer and Kloker [4]. The freestream temperature is $T^* = 220K$, and a cold isothermal wall with $T_{wall}^* = 975K \approx \frac{1}{2} T_{rec}^*$ is prescribed. At the wall, in TEQ holds $T_w^* = T_i^*{}^{vib}$, and the temperature disturbances are zero, $T'^* = T_i'^*{}^{vib} = 0$. The global Reynolds number is $Re_L = 10^5$ and the unit Reynolds number $Re_{unit}^* = 5.71 \cdot 10^6 \text{ 1/m}$, thus $L^* = 0.0175 \text{ m}$.

In figure 1a, the temperature profiles (left) of the baseflow are shown for all three models. At the inflow boundary the case TNEQ is set to case CPG. For the cases TEQ and TNEQ the maximum temperature in the boundary layer is smaller than

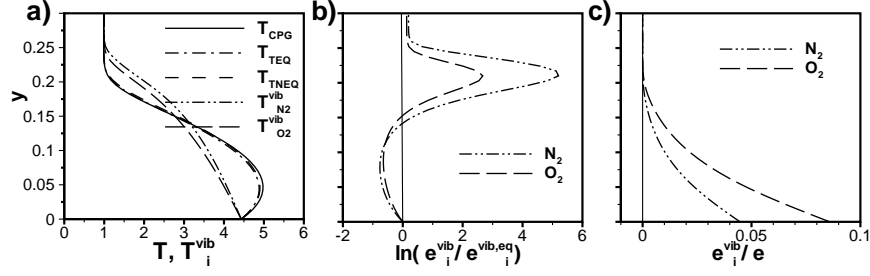


Fig. 1 Mach-6.8 boundary layer with various gas models (CPG: calorically perfect gas; TEQ: thermal equilibrium; TNEQ: thermal nonequilibrium) at $Re_x = 20 \cdot 10^5$: (a) temperature, (b) deviation of vibrational energies from equilibrium for case TNEQ, (c) vibrational energies for case TNEQ.

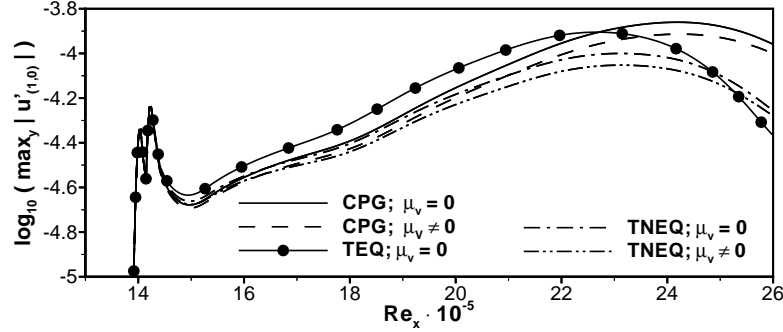


Fig. 2 Evolution of a linear 2-d disturbance wave (2^{nd} mode; $F = 10^{-4}$) for the different gas models with bulk viscosity μ_v turned on (eq. 4) or off.

in case CPG. The heat capacity c_v^* is a function of the temperature for TEQ, increasing with temperature. The deviation from equilibrium in case TNEQ is shown in figure 1b. The strongest nonequilibrium region is at the boundary-layer edge. However, the nonequilibrium energy is only a small fraction of the total energy e (Fig. 1c). The energy in the vibrational motion has its maximum at the wall, but only is approximately 13% of the total energy. Note that the effect of $\mu_v^* \neq 0$ is negligible for the baseflows.

The downstream development of the u -velocity amplitude for cases CPG, TEQ, and TNEQ is presented in figures 2 and 3. In a disturbance strip at $Re_x \approx 14.1 \cdot 10^5$ ($R_x = 1187$), an amplified 2-d 2^{nd} -mode disturbance (1,0) is introduced by blowing/suction. (h, k) indicates a wave with frequency $h \cdot F$ and the spanwise wavenumber $k \cdot \gamma$. The frequency parameter is $F = 2\pi f^* L^* / (u_\infty^* Re_L) = 10^{-4}$ ($f^* = 184 \text{ kHz}$). The influence of the different gas models and the bulk viscosity on the disturbance evolution is shown in Fig. 2. $\mu_v \neq 0$ always damps, and case TEQ shows the earliest amplitude decay after strongest growth, whereas TNEQ has the lowest initial growth. For the case shown in figure 3, the amplitude of (1,0) is increased, and a damped oblique 1^{st} -mode disturbance (1,1) is added. The spanwise wavenumber is $\gamma = 11$ ($\gamma^* = \gamma/L^* = 628.6/m$). The largest amplitude of (1,0) is reached in case CPG, and the originally damped 3-d disturbance (1,1) undergoes resonant amplification at $Re_x \approx 21 \cdot 10^5$. Somewhat further downstream, higher harmonics reach

high amplitudes as well and the fundamental breakdown begins. In case TNEQ, (1,1) gets in resonance as well, but the amplitude of (1,0) is smaller and hence the growing of the amplitude (1,1) is not as strong as for the other case. As a consequence, the fundamental-breakdown scenario eventually falls off. The scenario in the TEQ case is slightly weaker but similar to the CPG case.

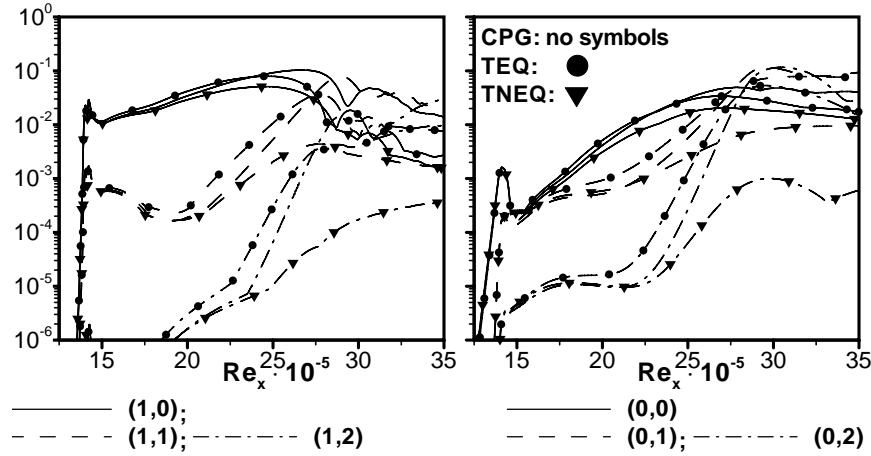


Fig. 3 Downstream development of $u'_{(h,k)}$ (wall-normal max.) in a Mach-6.8 boundary layer for the three gas models (CPG, TEQ: $\mu_v^* = 0$; TNEQ: $\mu_v^* \neq 0$).

3 Conclusions

DNS were performed to investigate the influence of different gas models on a fundamental-breakdown scenario at Mach 6.8 at flight conditions. Three different gas models were used namely calorically perfect gas (CPG), thermal equilibrium (TEQ), and thermal nonequilibrium (TNEQ). The baseflow shows only slight differences for the translational temperature profiles. The CPG and TEQ cases show approximately the same behavior for the fundamental-breakdown case, with lower amplitudes for case TEQ. For case TNEQ the growth rates of the disturbances are lower and breakdown does not occur. Albeit the influence of the gas models on the baseflow is small, their impact on the disturbance evolution can be significant.

References

1. Anderson, J.D. (1989) Hypersonic and High Temperature Gas Dynamics, MacGraw-Hill
2. Babucke, A., Linn, J., Kloker, M. and Rist, U. (2006). Direct numerical simulation of shear flow phenomena on parallel vector computers In: M. Resch, et al. (Eds.), *High Performance Computing on Vector Systems 2005*, pp. 229–247. Springer.
3. Bertolotti, F.B. (1998) The influence of rotational and vibrational energy relaxation on boundary-layer stability. *J. Fluid Mech.*, vol. 372, pp. 93-118.
4. Fezer, A., Kloker, M.J. (1999) Transition process in Mach 6.8 boundary layers at varying temperature conditions investigated by spatial direct numerical simulation. In: *New Results in Numerical and Experimental Fluid Mechanics II.*, W. Nitsche et al. (eds.) NNFM, vol. 72, Vieweg, pp. 138-145.